

Figure 3. Daily mean distribution of the (a) AI retrieved from the OMI satellite data and simulated optical depth of (b) dust aerosols and (c) carbonaceous and sulfate aerosols from 21 to 23 August 2007.

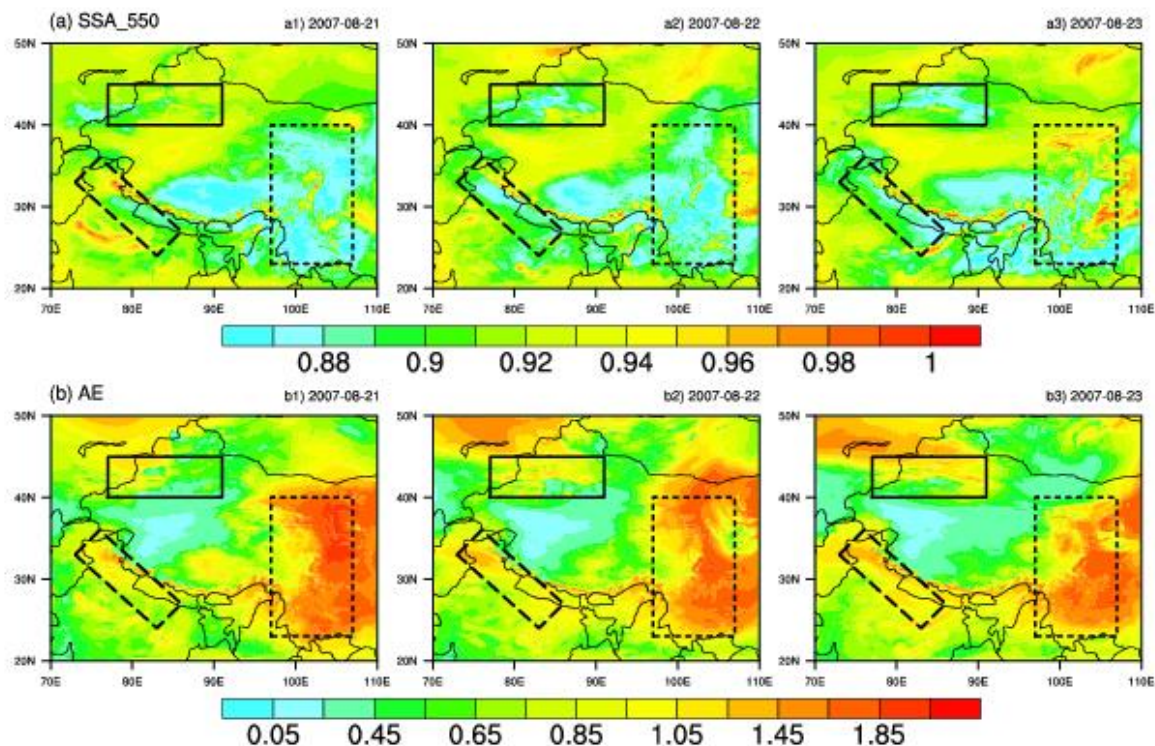


Figure 4. Simulated daily mean distributions of the (a) single scattering albedo and (b) Angstrom exponent from 21 to 23 August 2007. The black rectangles indicate three areas of interest.

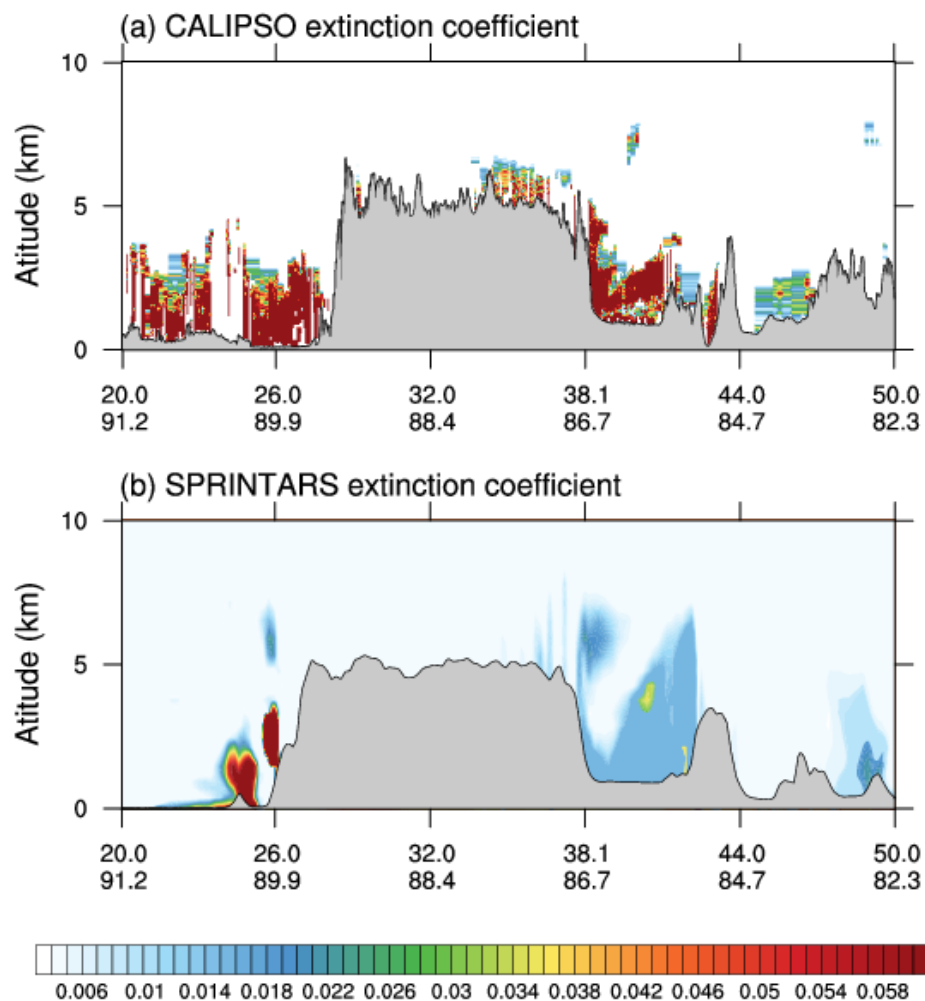


Figure 5. The vertical cross-section of the aerosol extinction coefficient (unit: km^{-1}) from (a) CALIPSO and (b) the simulation by SPRINTARS on 22 August 2007. The gray shading indicates the topography.

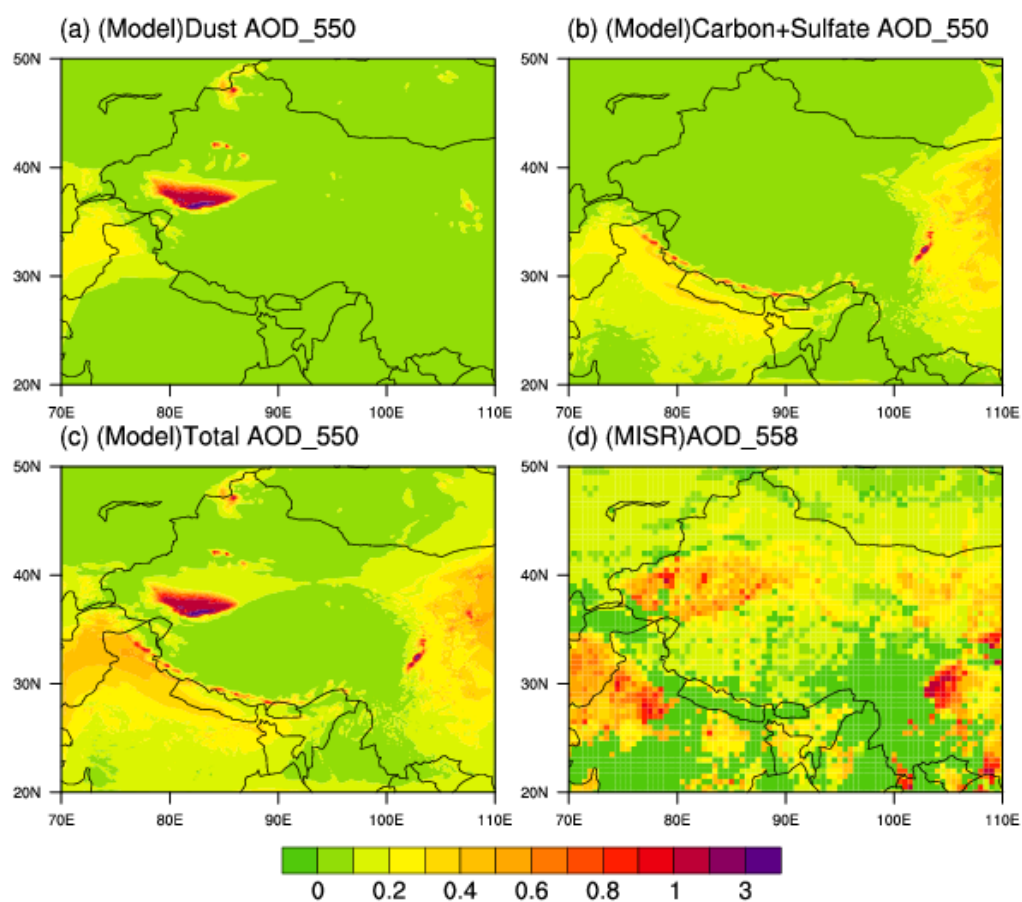


Figure 6. Monthly mean aerosol optical depths from the MISR and SPRINTARS simulations for August 2007.

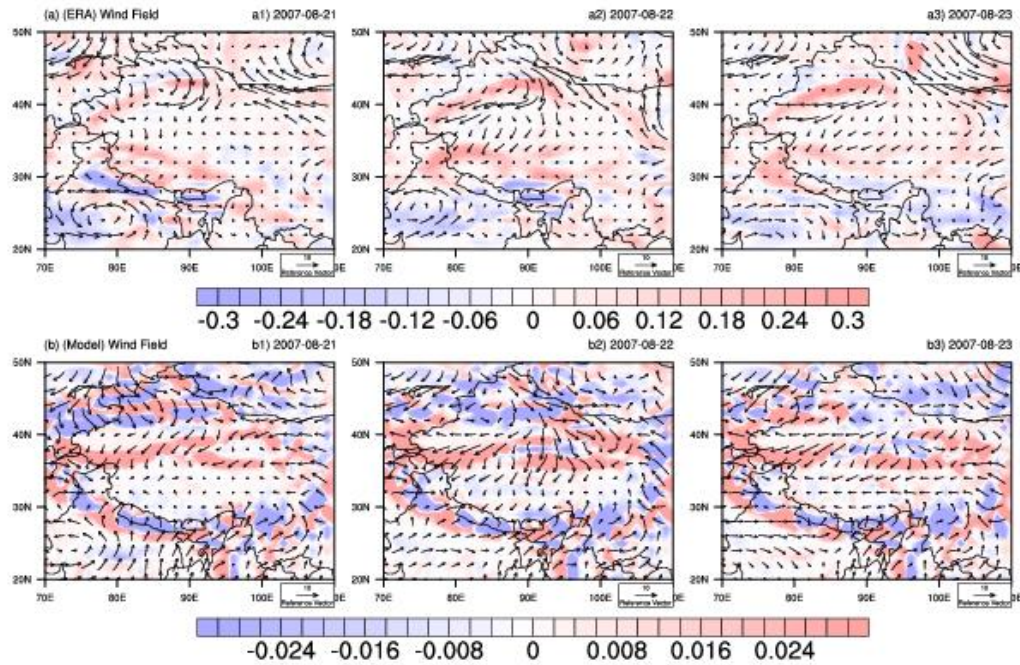


Figure 7. (a) Wind field from ERA-Interim at the 850 hPa level (arrows for the U and V components of the horizontal wind, units: ms^{-1} ; colors for the vertical wind velocity, the unit is Pas^{-1} and the values are negative for updrafts and positive for downdrafts) from 21 to 23 August 2007. **(b)** Same as **(a)** but for the simulated wind field at 20 m (units: m s^{-1} , the values of the vertical wind velocity are negative for downdrafts and positive for updrafts).

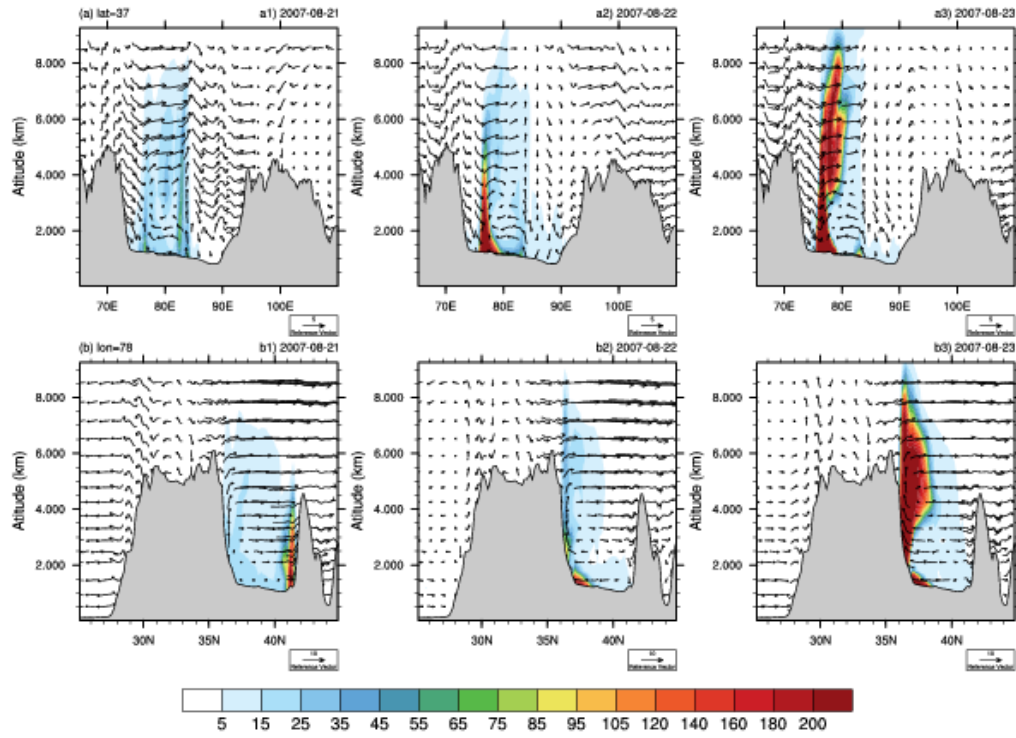


Figure 8. Cross-section of the (a) vertical-longitude and (b) vertical-latitude distributions of the simulated dust mass concentration (units: $\mu\text{g m}^{-3}$) and wind vectors (shown in arrows; the vertical velocity is multiplied by 10 and 30 for panels a and b, respectively) from 21 to 23 August 2007. The gray shading indicates the topography.

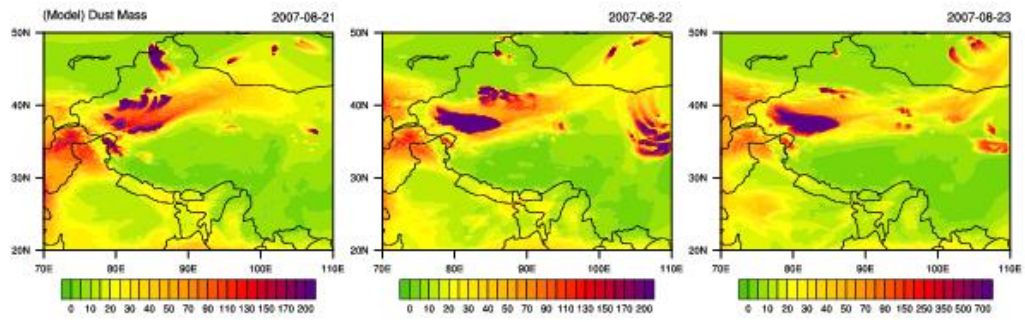


Figure 9. Distributions of the simulated dust mass column loading (units: mg m^{-2}) from 21 to 23 August 2007.